City Research Online

City, University of London Institutional Repository

This is the published version of the paper.

This version of the publication may differ from the final published version.

Permanent repository link: https://openaccess.city.ac.uk/id/eprint/32151/

Link to published version: https://doi.org/10.1002/jmrs.741

ORIGINAL ARTICLE

Effects of body part thickness on low-contrast detail detection and radiation dose during adult chest radiography

Sadeq Al-Murshedi, PhD[1,2], Kholoud Alzyoud, PhD[3], Mohamed Benhalim, PhD[4], Nadi Alresheedi PhD[5], Stamatia Papathanasiou, PhD[6], & Andrew England, PhD[7]

[1]College of Health and Medical Technology, AL-Zahraa University for Women, Karbala, Iraq
[2]Physics Department, College of Education for Pure Science, University of Babylon, Babil, Iraq
[3]Department of Medical Imaging, Faculty of Applied Health science, The Hashemite University, Zarqa, Jordan
[4]Collage of Medical Technology Misurata, Misurata, Libya
[5]Department of General studies, Royal Commission for Jubail and Yanbu, Yanbu Industrial College, Yanbu, Kingdom of Saudi Arabia
[6]City University of London, London, UK
[7]School of Medicine, University College Cork, Cork, Ireland

Abstract

Introduction: Differences in patient size often provide challenges for radiographers, particularly when choosing the optimum acquisition parameters to obtain radiographs with acceptable image quality (IQ) for diagnosis. This study aimed to assess the effect of body part thickness on IQ in terms of low-contrast detail (LCD) detection and radiation dose when undertaking adult chest radiography (CXR). **Methods:** This investigation made use of a contrast detail (CD) phantom. Polymethyl methacrylate (PMMA) was utilised to approximate varied body part thicknesses (9, 11, 15 and 17 cm) simulating underweight, standard, overweight and obese patients, respectively. Different tube potentials were tested against a fixed 180 cm source to image distance (SID) and automatic exposure control (AEC). IQ was analysed using bespoke software thus providing an image quality figure inverse (IQF_{inv}) value which represents LCD detectability. Dose area product (DAP) was utilised to represent the radiation dose. **Results:** IQF_{inv} values decreased statistically ($P = 0.0001$) with increasing phantom size across all tube potentials studied. The highest IQF_{inv} values were obtained at 80 kVp for all phantom thicknesses (2.29, 2.02, 1.8 and 1.65, respectively). Radiation dose increased statistically ($P = 0.0001$) again with increasing phantom thicknesses. **Conclusion:** Our findings demonstrate that lower tube potentials provide the highest IQF_{inv} scores for various body part thicknesses. This is not consistent with professional practice because radiographers frequently raise the tube potential with increased part thickness. Higher tube potentials did result in radiation dose reductions. Establishing a balance between dose and IQ, which must be acceptable for diagnosis, can prevent the patient from receiving unnecessary additional radiation dose.

Introduction

In diagnostic radiography, imaging larger size patients can present difficulties for radiographers.[1] Transportation, identifying anatomical landmarks, providing precise positioning and central ray location are a few of the challenges. Alongside and importantly, selecting the right acquisition parameters to provide the best image quality (IQ) is the primary objective.[2–5] The Commission of the European Communities (CEC) guidelines and many optimisation studies have focused on patients of a 'standard' or 'average' size rather than those of variable body habitus.[6–8] However, the prevalence of obesity is rising globally,[3] and radiographers will be more frequently required to adjust their imaging protocols to obtain adequate diagnostic IQ when imaging larger size patients.

X-ray attenuation, scattered radiation, motion artefacts and reductions in contrast all increase with the size of the imaged part. These are the product of longer exposure times.[3,9] Even with digital imaging systems that are designed to automatically compensate for an optimum image contrast (using AEC), this can still have an impact on IQ in obese patients.[10]

As a result of these developments, one question still remains – does increasing body part thickness affect low-contrast detail (LCD) detection when undertaking adult chest X-ray radiography (CXR) using automatic exposure control (AEC)? If body part thickness has an influence on LCD detection, this could impact pathology detection in clinical practice. The purpose of this research was to determine how the thickness of different body parts affected the IQ (represented by IQF_{inv}) of adults undergoing a chest X-ray. IQF_{inv} values are a new method for reporting IQ (measuring LCD detectability using a CDRAD 2.0 phantom). This has several distinct advantages compared with previous methods described within the literature and will be explained in the Methods section.

Methods

Imaging equipment and technique

An X-ray machine (Willenhall, West Midlands, UK)) with 3 mm Al total filtration and a Caesium Iodide (CsI) detector was used. This DR system included an AeroDR detector (Konica Minolta Medical Imaging USA INC, Wayne, NJ) with a 1994 × 2430 pixel matrix (175 µm pixel size). Imaging included the use of a stationary anti-scatter grid (10:1 ratio, 40 lines/cm frequency). The X-ray machine passed IPEM Report 91 quality control tests.[11]

Four thicknesses (9, 11, 15 and 17 cm) of Polymethyl methacrylate (PMMA) were added in front and behind a CDRAD 2.0 phantom (Artinis Medical System, The Netherlands) (Fig. 1A and B).[12] The PMMA was used to represent different body part thicknesses of the chest region for underweight, standard size, overweight and obese patients, respectively. The primary X-ray beam was collimated to the boundaries of the CDRAD 2.0 phantom and was focused on the centre of the phantom.

Automatic exposure control (AEC), using three AEC chambers, was used to acquire radiographs at various tube potentials (kVp) settings, and at a source-to-image distance (SID) of 180 cm. The tube potentials (kVp values) used and resulting tube current-time-product (mAs) values for various phantom sizes are summarised in Table 1. These imaging parameters were based on those used in clinical practice and the literature.[13] Image post-processing was based on a posteroanterior chest algorithm selected within the DR system.

In total, 44 radiographs were generated (11 radiographs for each phantom size); three repeat radiographs were acquired by imaging the phantom three times for each
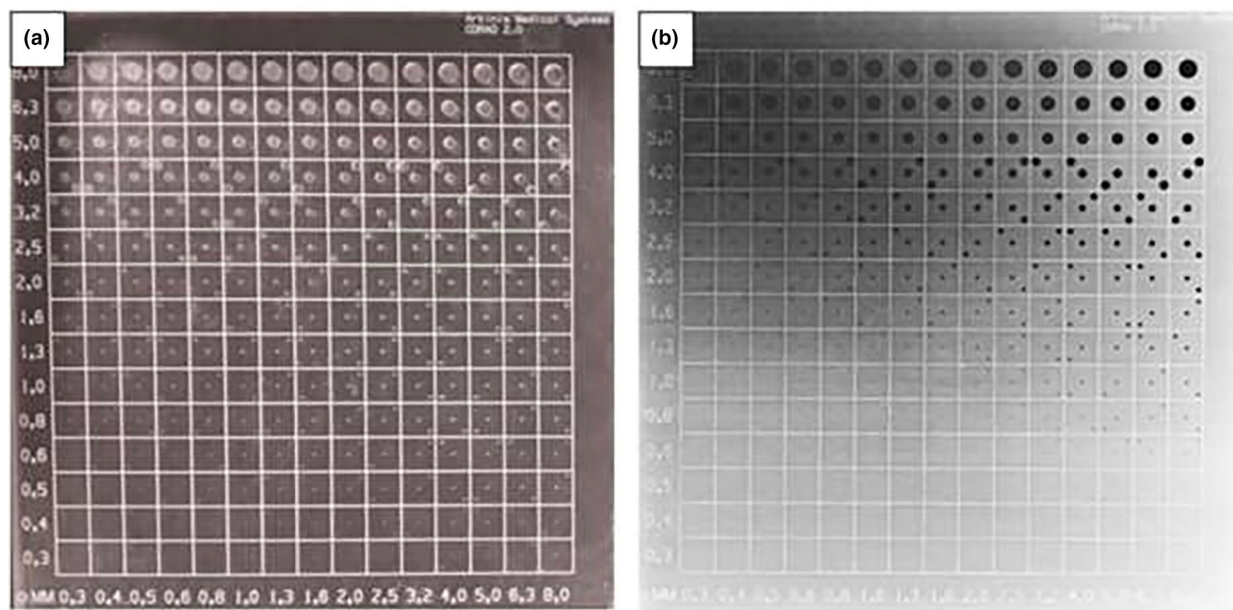

Figure 1. Photograph of the CDRAD 2.0 phantom (A) and the resultant radiographic image of the CDRAD 2.0 phantom (B). The phantom is a 1 cm-thick PMMA slap with round holes ranging from 0.3 to 8.0 mm in size and depth. These holes are in 15 rows of increasing size and 15 columns of increasing contrast (depth). Each of the 225 squares has one or two random holes in the centre and corners.

Table 1. lists the exposure parameters that were utilised to acquire radiographs of the various phantom sizes.

Image no.	kVp	Underweight mAs*	Standard size mAs*	Overweight mAs*	Obese mAs*
1	80	4	6.2	14.4	21
2	85	3.2	4.8	10.7	16.1
3	90	2.5	3.6	8.1	12.1
4	95	2	2.8	6.2	9.2
5	100	1.7	2.5	5.1	7.5
6	105	1.4	2	4.3	6.4
7	110	1.2	1.9	3.6	5.2
8	115	1.2	1.7	3.3	6.4
9	120	1.1	1.6	2.8	4.1
10	125	0.9	1.4	2.5	3.6
11	130	0.9	1.2	2.4	3.3

*The values represent the mean of the three mAs values (the same reading was recorded during the three repeat exposures).

parameter settings based on the vendor of CDRAD 2.0 recommendations.[9]

Image quality evaluation and dose measurement

Image quality figure inverse (IQF_{inv}) values (which indicate an ability to identify small objects against a low-contrast background) represent the LCD detection resulting from the CDRAD 2.0 phantom images and were assessed using the CDRAD 2.0 analyser software and calculated using equation 1,

$$IQF_{inv} = \sum_{i=1}^{15} \frac{1}{C_i D_{(i,th)}} \qquad (1)$$

$D_{(i, th)}$ and C_i refer to the threshold diameter and contrast in column (i) that were identified correctly, respectively.

The advantages of using the CDRAD 2.0 phantom are that it makes it possible to thoroughly assess radiographic noise, sharpness and contrast. Improved IQF_{inv} values in clinical practice could improve the identification of subtle diseases, for example, small lung nodules.[14,15] Moreover, a physical IQ method was used for calculating IQF_{inv} using CDRAD 2.0 analyser software which offers high reliability and is unaffected by differences in human eyesight and experience.[16] The CDRAD 2.0 phantom and IQF_{inv} measurements have been used widely for optimization studies and when comparing different DR detector types.[17–20] Studies reported a strong relationship with visual IQ when evaluating lesion visibility, especially for CXR.[21–23]

The radiation dose recorded from Dose Area Product (DAP) was measured three times for each exposure to reduce random error.

Statistical analysis

The normality of the data for both IQF_{inv} and DAP values was investigated using the Shapiro–Wilk test. A Kruskal–Wallis test (for non-parametric data) was used to compare the values of IQF_{inv} and radiation dose resulting from the range of tube potentials used among the different phantom sizes (9, 11, 15 and 17 cm). Statistical analysis was performed using SPSS (IBM Inc, Armonk, NJ).

Results

Figures 2 and 3 show the radiation dose and IQF_{inv} values for the four phantom thicknesses (9, 11, 15 and 17 cm), respectively. Kruskal–Wallis test results demonstrated that there is a statistically significant difference in IQF_{inv} values ($P = 0.0001$) between the different body part thicknesses (underweight, standard, overweight and obese). Similar to this, according to Kruskal–Wallis test results there was a statistically significant difference ($P = 0.0001$) in radiation dose values between the different phantom thicknesses.

Figure 3 clearly shows that IQF_{inv} values decreased statistically ($P = 0.0001$) with increasing phantom thicknesses across the different tube potentials. In addition, IQF_{inv} values are higher for lower tube potential settings for all phantom thicknesses. In contrast, radiation dose (Fig. 2) increased statistically ($P = 0.0001$) with increasing phantom thicknesses and for lower tube potentials where higher dose values were observed.

Underweight, standard size, overweight and obese phantom sizes generated mean IQF_{inv} values of 1.81, 1.55, 1.39 and 1.33, respectively; while their corresponding mean radiation dose values were 25.5, 37.2, 78.2 and 115.7 mGy.cm^2.

Discussion

The influence of body part thickness, under various tube potentials, on IQ (IQF_{inv} values) and radiation dose during adult CXR was evaluated. The findings of our study suggest that radiographic techniques could be further modified when imaging larger patients.

In our study, increasing phantom thicknesses reduced CXR IQF_{inv} values for all tube potentials studied since increasing the body part thickness increases X-ray beam attenuation and scatter and thus decreases contrast. Generally, IQF_{inv} values increased as tube potential was reduced, the highest value was recorded at 80 kVp for all body part thicknesses. This trend does not correspond with standard clinical practice when radiographers frequently raise the tube potential as body part thickness rises. This is because lower energy photons are attenuated
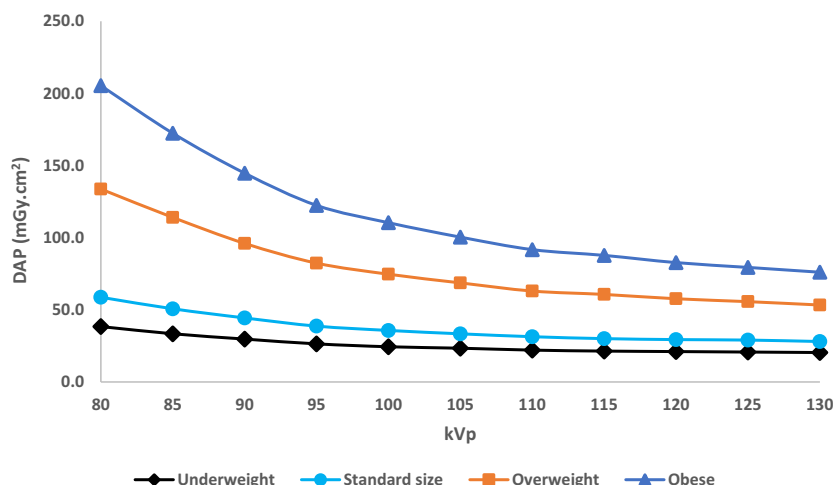
Figure 2. Comparison of radiation dose values for different phantom thicknesses (9, 11, 15 and 17 cm) across a range of different tube potentials.
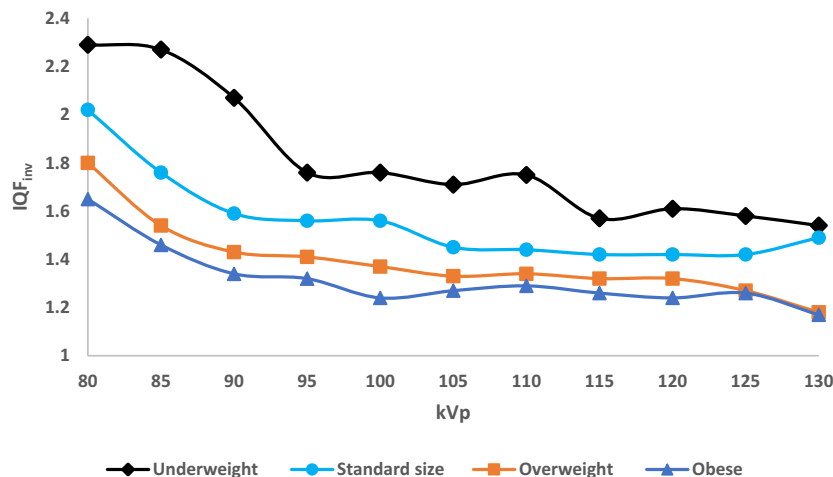

Figure 3. Comparison of IQF_{inv} values for different phantom thicknesses (9, 11, 15 and 17 cm) across a range of different tube potentials.

more than higher energy photons, which increases contrast for low-contrast objects and image contrast as photon energy decreases (reducing kVp).

According to the authors' knowledge, this is the first such study to investigate the impact of body part thickness on LCD detection using the CDRAD 2.0 phantom when undertaking adult CXR, and then comparing this to existing literature is challenging. Even so, we are still able to summarise findings from other studies that investigated how different body part thicknesses affected IQ for different anatomical areas when using a range of methodologies.

Alzyoud and colleagues[24] demonstrated the effect of body part thicknesses (1–15 cm of animal fat) on IQ and radiation dose when undertaking pelvis radiography. IQ

was evaluated visually using a visual grading analysis (VGA) method and physically using signal-to-noise ratio (SNR) and contrast to noise ratio (CNR). The authors found that the physical and visual IQ decreased when increasing the thickness of the phantom and the radiation dose increased similarly. Lower tube potential values (70 kVp) were found to have the highest IQ and the lowest IQ was found at 110 kVp, still delivering acceptable images for diagnosis. These findings were concurred in studies by Gatt et al.[25] and Kawashima and colleagues.[26]

Gatt et al.[25] compared the IQ and radiation dose (DAP values) for different body part thicknesses when undertaking a posteroanterior (PA) abdomen X-ray examination, IQ was assessed both visually (VGA method) and physically (SNR and CNR). They found that with

increasing part thicknesses, radiation doses increased whereas IQ decreased; again the highest IQ values were observed at lower kVp values (80 kVp), while 110 and 120 kVp were considered the optimal protocol that produced acceptable IQ with the lowest radiation dose. The same results were found during our current study focusing on the chest region, where the DAP was found the highest at lower tube potentials.

A study by Kawashima and colleagues[27] demonstrated the influence of part thicknesses (10, 15, 20, 25 cm) on IQF_{inv} during abdomen radiography and they found that IQF_{inv} decreased with increasing phantom thicknesses. However, the study was designed for abdomen radiography and each phantom thickness was imaged with only one exposure at 80 kVp. Other tube potentials were not examined and then it was not possible to fully investigate the relationship between the body part thicknesses and IQF_{inv} across a range of acquisition parameters used in clinical practice.

A study by Moore et al.[28] investigated the optimal acquisition parameters during computed radiography (CR) adult CXR for average-size and obese patients utilising a computer simulator for a digitally created radiograph. They found that visual IQ (VGA method) was increased at low tube potentials for both average and obese size patients. The result from our study is also comparable with Moore et al.[15]

Our study's findings are comparable with those of Alzyoud and colleagues,[24] Gatt et al.,[25] Kawashima and colleagues[26] and Moore et al.[28] despite the fact that the techniques, IQ types, phantom types and thicknesses and imaging protocols differed.

Our study has a limitation because we only employed a single image detector. Future research might examine other DR and CR system types. Radiation dose was evaluated using DAP, calculations of the effective dose are likely to more realistically represent the radiation dose to the patient. In our study, modifications to acquisition parameters only considered tube potential; however, a thorough optimization study for differences in body habitus should take into account the combination of kVp and mAs, changes in SID, and additional filtration. Fat modelling by adding PMMA was used as an additional soft tissue in this experiment; however, fat distribution in the human body does not always take the same form. Future research should take into account the wide range of shapes of people who are overweight or obese.

Conclusion

IQF_{inv} values decreased significantly with increasing body part thickness with the highest values of IQF_{inv} observed at lower tube potentials (80 and 85 kVp). This is contrary

to professional practice, where practitioners frequently raise tube potential with increasing patient thickness. This is an important finding and radiographers should consider this when optimising examinations on a per-patient basis. Furthermore, prior to the imaging, the radiographer should review the clinical indications to help determine the optimal tube potential. If the clinical problem requires a high level of LCD detection, such as the detection of subtle lesions then lower tube potentials might be beneficial but with the acceptance of a higher radiation dose. Further clinical and perceptual research studies are essential, but practitioners should consider utilising lower tube potentials for larger patient sizes during adult CXR.

Conflict of interest

The author declares no conflict of interest.

Acknowledgments

Ethical approval

This research does not involve human participants and animals.

Data availability statement

Data available on request from the authors.

References

1. Tugwell JR, England A, Hogg P. Antero-posterior (AP) pelvis x-ray imaging on a trolley: Impact of trolley design, mattress design and radiographer practice on image quality and radiation dose. *Radiography* 2017; **23**: 242–8.

2. Reynolds A. Obesity and medical imaging challenges. *Radiol Technol* 2011; **82**: 219–39.

3. Carucci LR. Imaging obese patients: Problems and solutions. *Abdom Imaging* 2013; **38**: 630–46.

4. Glanc P, O'Hayon BE, Singh DK, Bokhari SAJ, Maxwell CV. Challenges of pelvic imaging in obese women. *RadioGraphics* 2012; **32**: 1839–62.

5. Yanch JC, Behrman RH, Hendricks MJ, McCall JH. Increased radiation dose to overweight and obese patients from radiographic examinations. *Radiology* 2009; **252**: 128–39.

6. Commission of the European Communities (CEC). European Guidelines on Quality Criteria for Diagnostic Radiographic Images: (EUR 16260 EN). CEC, Luxembourg, 1996. Available from: https://publications.europa.eu/en/publication-detail/-/publication/d59ccc60-97ed-4ce8-b396-3d2d42b284be/language-en.

7. Moore CS, Wood TJ, Avery G, et al. Investigating the use of an antiscatter grid in chest radiography for average adults with a computed radiography imaging system. *Br J Radiol* 2015; **88**(1047): 20140613.

8. Lorusso JR, Fitzgeorge L, Lorusso D, Lorusso E. Examining practitioners' assessments of perceived aesthetic and diagnostic quality of high kVp-Low mAs pelvis, chest, skull, and hand phantom radiographs. *J Med Imaging Radiat Sci* 2015; **46**: 162–73.

9. Shah S, Shah V, Ahmed AR, Blunt DM. Imaging in bariatric surgery: Service set-up, post-operative anatomy and complications. *Br J Radiol* 2011; **84**: 101–11.

10. van den Heuvel J, Punch A, Aweidah L, Meertens R, Lewis S. Optimizing projectional radiographic imaging of the abdomen of obese patients: An e-Delphi study. *J Med Imaging Radiat Sci* 2019; **50**: 289–96.

11. Institute of Physics and Engineering in Medicine. IPEM Report 91: Recommended Standards for the Routine Performance Testing of Diagnostic x-ray Imaging Systems. IPEM, York, 2005.

12. van der Burght R, Floor M, Thijssen M, Bijkerk R. Manual CDRAD 2.0 phantom and analyser software version 2.1. Artinis Medical Systems, The Netherlands. Einsteinweg 17, Artinis Medical Systems, The Netherlands, 2014.

13. Al-Murshedi S, Hogg P, England A. Relationship between body habitus and image quality and radiation dose in chest X-ray examinations: A phantom study. *Phys Med* 2019; **57**: 65–71.

14. Fujita H, Kuwahata N, Hattori H, Kinoshita H, Fukuda H. Investigation of optimal display size for viewing T1-weighted MR images of the brain using a digital contrast-detail phantom. *J Appl Clin Med Phys* 2016; **17**: 353–9.

15. Saito K, Hiramoto S, Gomi T, et al. Evaluation of chest and abdominal exposure dose appropriate for a digital image reader system incorporating a columnar-crystal structured phosphor plate and a contrast-detail phantom. *Radiol Phys Technol* 2008; **1**: 238–43.

16. Pascoal A, Lawinski CP, Honey I, Blake P. Evaluation of a software package for automated quality assessment of contrast detail images—comparison with subjective visual assessment. *Phys Med Biol* 2005; **50**: 5743–57.

17. Al-Murshedi S, Hogg P, Meijer A, Erenstein H, England A. Comparative analysis of radiation dose and low contrast detail detectability using routine paediatric chest radiography protocols. *Eur J Radiol* 2019; **113**: 198–203.

18. Al-Murshedi S, Hogg P, Lanca L, England A. A novel method for comparing radiation dose and image quality, between and within different X-ray units in a series of hospitals. *J Radiol Prot* 2018; **38**: 1344–58.

19. Enevoldsen S, Kusk MW. Image quality of bedside chest radiographs in intensive care beds with integrated detector tray: A phantom study. *Radiography* 2021; **27**: 453–8.

20. Precht H, Outzen CB, Kusk MW, Bisgaard M, Waaler D. Comparison of conventional hand examination on six optimised DR systems. *Radiat Prot Dosimetry* 2021; **194**: 27–35.

21. De Crop A, Bacher K, Van Hoof T, et al. Correlation of contrast-detail analysis and clinical image quality assessment in chest radiography with a human cadaver study. *Radiology* 2012; **262**: 298–304.

22. Al-Murshedi S, Hogg P, England A. An investigation into the validity of utilising the CDRAD 2.0 phantom for optimisation studies in digital radiography. *Br J Radiol* 2018; **91**: 20180317.

23. Al-Murshedi S, Benhalim M, Alzyoud K, Papathanasiou S, England A. Relationship between the visual evaluation of pathology visibility and the physical measure of low contrast detail detectability in neonatal chest radiography. *Radiography* 2022; **28**: 1116–21.

24. Alzyoud K, Hogg P, Snaith B, Flintham K, England A. Impact of body part thickness on AP pelvis radiographic image quality and effective dose. *Radiography* 2018; **25**: 1–7.

25. Gatt S, Portelli JL, Zarb F. Optimisation of the AP abdomen projection for larger patient body thicknesses. *Radiography* 2022; **28**: 107–14.

26. Kawashima H, Ichikawa K, Hanaoka S, Matsubara K. Optimizing image quality using automatic exposure control based on the signal-difference-to-noise ratio: A phantom study. *Australas Phys Eng Sci Med* 2019; **42**: 803–10.

27. Platin E, Mauriello S, Ludlow JB. Effects of focal spot size on caries diagnosis with D and e speed images. *Oral Surg Oral Med Oral Pathol Oral Radiol Endod* 1996; **81**: 235–9.

28. Moore CS, Avery G, Balcam S, et al. Use of a digitally reconstructed radiograph-based computer simulation for the optimisation of chest radiographic techniques for computed radiography imaging systems. *Br J Radiol* 2012; **85**: e630–9.